

Second excited state of ^4He tetramer

A. Deltuva

Institute of Theoretical Physics and Astronomy, Vilnius University, Saulėtekio al. 3, LT-10257 Vilnius, Lithuania
(Received October 13, 2025)

The four-boson universality suggests the existence of the second excited tetramer state in a system of cold ^4He atoms. It is not bound but could be seen as a resonance in the atom-trimer scattering. This process is rigorously calculated using the momentum-space transition operator framework with two realistic interatomic potentials. The S -wave phase shift and cross section show a resonant behavior below the excited trimer threshold, but there are sizable nonresonant contributions from P and D waves as well. The position and width of the resonant state is determined, for the latter significant finite-range effects are found.

I. INTRODUCTION

The few-body systems of atomic ^4He atoms are among the best known examples for the natural realization of the Efimov physics [1, 2]. The two-atom scattering length a is large compared to the range of the interatomic van der Waals interaction r_{vdW} and the effective range, supporting only one very weakly bound two-body state in the S -wave, the dimer with the binding energy $B_2 \sim \hbar^2/m_a a^2 \sim 1 \text{ mK}$, m_a being the mass of the atom. Consequently [3–5], several weakly bound states should exist also in the systems consisting of three and four ^4He atoms. Indeed, a number of calculations using realistic interaction models [6, 7] predicted two states of the trimer [8–16], a deep one with the binding energy $B_3 \sim 100 B_2$, and a shallow one close to the atom-dimer threshold, $B_2 < B_3^* < 2 B_2$. Similarly, two bound states were predicted also in the four-atom system [8, 10, 14, 15, 17], one deep and one shallow, close to the atom-trimer threshold. In the latter case there are significant differences in predicted binding energies, with only three most advanced calculations [10, 15, 17] being in a reasonable agreement. The above-mentioned tetramer states are associated with the trimer ground state, their binding energies roughly being $B_4 \sim 4.5 B_3$ and $B_4^* \sim 1.01 B_3$, respectively.

In the ideal Efimov scenario there should be two tetramer states associated with each trimer state [18–20]. The tetramers associated with the excited states of the trimer are not truly bound states, but resonant-like unstable bound states (UBS) residing in the continuum [21, 22]. Their properties have been calculated with high accuracy using simple separable potentials [20, 22, 23]. The results of Ref. [23] suggest that for B_3^*/B_2 values corresponding to a realistic ^4He atomic system there is only one associated physically observable tetramer, the deeper one. When increasing $1/a$ from the unitary limit toward the physical point the shallow tetramer turns into a virtual state through the dimer-dimer threshold and moves far away from the physical region, therefore becoming unobservable. The schematic representation of energy levels and thresholds in the ^4He four-atom system is displayed in Fig. 1

For a realistic system of ^4He atoms the second excited

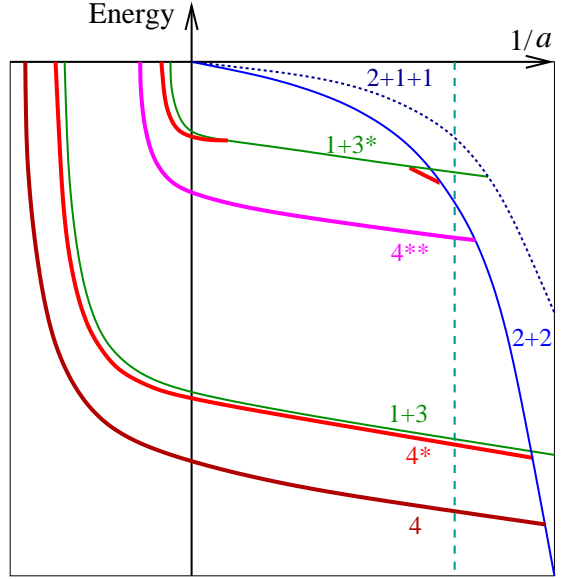


FIG. 1. (Color online) Schematic Efimov plot for the system of four ^4He atoms, i.e., the energy levels and thresholds as functions of the inverse two-atom scattering length. Only two families of states are shown. The energies of tetramers are displayed by thick curves; those labeled 4, 4^* and 4^{**} correspond to the ground, first and second excited states, respectively. The thin curves correspond to few-cluster thresholds. The vertical dashed line labels the physical ^4He point.

tetramer state has never been calculated. There are two main difficulties related: (i) the state is not a bound state but the atom-trimer scattering state located high above the two-cluster threshold, while the absolute majority of ^4He four-body calculations are for bound states [8, 14, 15] or in the vicinity of the atom-trimer threshold [10]; (ii) the realistic interaction between two ^4He atoms has weakly attractive van der Waals tail and very strong short-distance repulsion [6, 7, 24], that make the numerical solution highly challenging and very sensitive to fine details, especially for spatially extended states. These difficulties have been overcome recently using Alt, Grassberger, and Sandhas (AGS) equations [25] for the four-particle transition operators together with the “softening and extrapolation” method [17], where the strength

of the short-range repulsion was gradually reduced, enabling accurate solutions of dynamical equations, with subsequent extrapolation of the results back to the original potential. Solving four-body equations in the momentum space, Ref. [17] obtained not only tetramer binding energies but also atom-trimer and dimer-dimer scattering lengths.

The aim of the present work is to apply the momentum-space method from Ref. [17] to the atom-trimer scattering calculation near the excited trimer threshold and extract the properties of the resonant state, the second excited state of the tetramer. Further conclusions will be drawn regarding its observability, model dependence, and the importance of the finite-range effects.

Section II shortly recalls the description of the four-body scattering using transition operators together with the essential aspects of calculations. Section III presents results for the atom-trimer scattering in the vicinity of the resonant state. Discussion and conclusions are collected in Sec. VI.

II. ATOM-TRIMER SCATTERING EQUATIONS

The AGS equations [25] can be considered an integral version of the Faddeev-Yakubovsky equations [26]. While the latter are formulated for wave-function components, the AGS equations

$$\mathcal{U}_{11} = P_{34}(G_0 t G_0)^{-1} + P_{34} U_1 G_0 t G_0 \mathcal{U}_{11} + U_2 G_0 t G_0 \mathcal{U}_{21}, \quad (1a)$$

$$\mathcal{U}_{21} = (1 + P_{34})(G_0 t G_0)^{-1} + (1 + P_{34}) U_1 G_0 t G_0 \mathcal{U}_{11}, \quad (1b)$$

relate the four-particle transition operators $\mathcal{U}_{\beta\alpha}$ to the two-particle transition operator

$$t = v + v G_0 t \quad (2)$$

and 3+1 and 2+2 subsystem transition operators

$$U_\alpha = P_\alpha G_0^{-1} + P_\alpha t G_0 U_\alpha. \quad (3)$$

The above equations assume the bosonic symmetry, v is the two-particle potential,

$$G_0 = (E + i0 - H_0)^{-1} \quad (4)$$

is the free four-body resolvent at the available system energy E , and H_0 is the kinetic energy operator. The Greek subscripts $\alpha = 1$ (2) label the 3+1 (2+2) clustering, $P_1 = P_{12} P_{23} + P_{13} P_{23}$ and $P_2 = P_{13} P_{24}$, where P_{ab} is the permutation operator of particles a and b .

The AGS equations (1) are solved in the momentum-space partial-wave representation $|k_x k_y k_z [(l_x l_y) j l_z] JM \rangle_\alpha$, becoming an integral equation system with three continuous variables k_x, k_y, k_z that are the magnitudes of Jacobi momenta [27]. After their

TABLE I. Calculated dimer and trimer binding energies in units of mK. The numerical error is at most 1 in the last significant digit. The last line contains LM2M2 results obtained with $l_x, l_y \leq 8$.

	B_2	B_3^*	B_3
PCJS	1.6125	2.646	131.58
LM2M2	1.3094	2.277	126.30
LM2M2(8)	1.3094	2.278	126.50

discretization a large system of linear algebraic equations is obtained. The orbital angular momenta l_x, l_y, l_z are associated with the Jacobi momenta k_x, k_y, k_z . They are coupled to the total angular momentum J with the projection M , whereas j is an intermediate angular momentum. More details on the solution methods can be found in Refs. [17, 27].

Partial-wave amplitudes for the atom-trimer scattering are calculated as on-shell matrix elements

$$\mathcal{T}_J(E) = 3\langle \phi p J | \mathcal{U}_{11} | \phi p J \rangle \quad (5)$$

of the transition operator \mathcal{U}_{11} between the channel states $|\phi p J\rangle$ [27]. These states are direct products of the trimer ground state Faddeev amplitude ϕ and a free wave for the atom-trimer motion with total angular momentum J and relative two-cluster momentum p , related to the total energy $E = -B_3 + p^2/2\mu$, $\mu = 3m_a/4$ being the reduced mass. The factor 3 in Eq. (5) stems from the symmetrization.

This scattering amplitude is related to the single-channel S -matrix and scattering phase shift δ_J in a standard way, i.e.,

$$\mathcal{S}_J(E) = e^{2i\delta_J(E)} = 1 - 2i\pi\mu p \mathcal{T}_J(E). \quad (6)$$

Note that parity of the channel states is given by $\Pi = (-1)^J$ since the trimer has total spin zero.

III. RESULTS

The results are obtained using two realistic interatomic ${}^4\text{He}$ potentials. The older parametrization LM2M2 by Aziz and Slaman [6] is widely used for benchmarks, while that by Przybytek et al. (PCJS) [24] is among the most recent and sophisticated ones. They differ by about 20% in B_2 and B_3^* predictions, thereby allowing to explore the model dependence. As all realistic ${}^4\text{He}$ potentials, they have weakly attractive van der Waals tail and strong repulsion at short distances; this difficulty is reliably handled using the “softening and extrapolation” method from Ref. [17]. The calculations include partial waves with $l_x, l_y, l_z \leq 6$, where the trimer excited (ground) state binding energies are converged better than within 0.1% (0.2%). The $\hbar^2/m_a = 12.11928 \text{ \AA}^2$ value recommended in Ref. [13] is adopted. Table I collects the values for dimer and trimer binding energies.

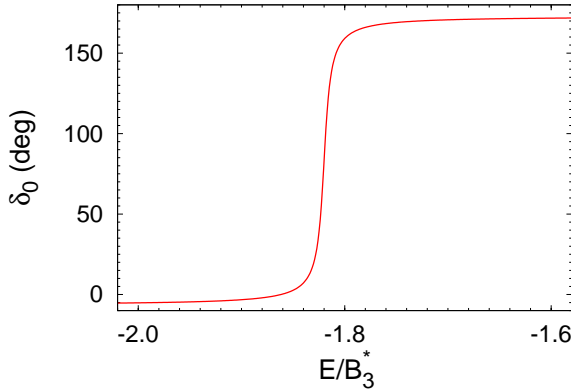


FIG. 2. (Color online) Energy dependence of the $J = 0$ phase shift for the LM2M2 interaction model in the vicinity of the second excited tetramer state.

Solving the atom-trimer scattering equations (1) and calculating the phase shift (6) reveals a very clear resonant behavior in the $J = 0$ state around the energy $E \approx -1.8 B_3^*$. It turns out that in this region the phase shift can be very well parametrized as a sum of slowly-varying background and resonant contributions [28], i.e.,

$$\delta_J(E) = \varphi_0 + \varphi_1 \frac{E}{B_3^*} + \arcsin \left[\frac{\Gamma/2}{\sqrt{(E + B_4^{**})^2 + (\Gamma/2)^2}} \right]. \quad (7)$$

Here B_4^{**} parametrizes the position of the resonance below the threshold of four free particles, while Γ is its width, i.e., in the complex energy plane the pole of the four-particle S -matrix and transition operators is located at $-B_4^{**} - i\Gamma/2$. The phase shift for the LM2M2 potential is shown in Fig. 2, where the values of parameters in Eq. (7) are $\varphi_0 = -7.8(1)$ deg, $\varphi_1 = -0.51(3)$ deg, $B_4^{**}/B_3^* = 1.82(2)$, and $\Gamma/B_3^* = 0.010(1)$. Since the second excited tetramer state is associated with the first excited trimer, B_3^* is chosen as the most natural energy scale in Eq. (7). Nevertheless, one could use B_3 as well taking the ratio from Table I.

The contribution of the $J = 0$ state to the total cross section

$$\sigma_J(E) = 4\pi(2J + 1) \frac{\sin \delta_J(E)}{p^2} \quad (8)$$

is shown in Fig. 3, exhibiting a sharp resonant peak, where the cross section rises by a factor of 100 as compared to the background.

However, one has to keep in mind that the considered regime is relatively high above the atom-trimer threshold and therefore other partial waves with $J > 0$ contribute as well. They do not show any resonant behavior, the corresponding phase shifts and cross sections do not change significantly in the considered regime. Their values at the $J = 0$ resonance energy are collected in Table II. It

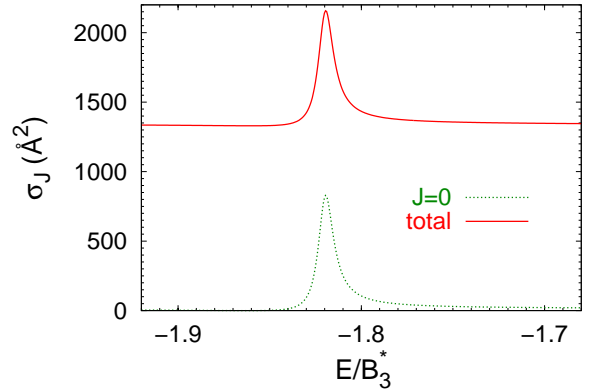


FIG. 3. (Color online) The total cross section and its $J = 0$ contribution as functions of energy calculated using the LM2M2 interaction model in the vicinity of the second excited tetramer state.

appears that $J = 1$ and $J = 2$ waves at this energy have appreciable values of phase shifts and cross sections, in the $J = 1$ case even exceeding the resonant contribution. In contrast, in $J = 3$ and higher waves the phase shifts in absolute values are below 1 deg, with entirely insignificant contributions to the total cross section, below 1 Å^2 .

TABLE II. Phase shifts and contributions to the total cross section at the energy corresponding to the $J = 0$ cross section peak. Results are obtained using the LM2M2 potential.

J	δ_J (deg)	σ_J (Å^2)
0	90.0(1)	830(1)
1	-41.1(1)	1076(3)
2	14.3(1)	253(2)

The calculations using the PCJS potential [24] yield very similar results. The extracted B_4^{**}/B_3^* , and Γ/B_3^* values are collected in Table III.

TABLE III. Position and width of the second excited tetramer state in ratio to the excited trimer binding energy. The universal results correspond to the $B_3^*/B_2 = 1.74$ ratio of the LM2M2 potential.

	B_4^{**}/B_3^*	Γ/B_3^*
PCJS	1.79(2)	0.009(1)
LM2M2	1.82(2)	0.010(1)
Universal	1.888(1)	0.0048(1)

IV. DISCUSSION AND CONCLUSIONS

The universal Efimov scenario predicts the existence of the second excited tetramer state in a realistic system of cold ^4He atoms. Being well above the atom plus ground-state trimer threshold, this state is an unstable bound state in the continuum that can be seen as a resonance in atom-trimer collisions. The difficulties in handling the four-particle scattering with van der Waals plus strongly repulsive potentials have been overcome by using the momentum-space transition operator framework together with the “softening and extrapolation” method [17].

The resonant behavior is very clearly pronounced in the $J = 0$ state. However, higher total angular momentum states significantly contribute to the nonresonant cross section, such that the increase of the total atom-trimer cross section at the peak is about 60% as shown in Fig. 3. This should be observable, although less dramatic than peaks predicted for the recombination at threshold [19, 29], dominated by the single $J = 0$ state.

Another important question is the size of finite-range

effects for realistic interatomic ^4He potentials, as compared to the strictly universal (zero-range) Efimov scenario. The latter results can be obtained from Ref. [23], and are listed in Table III. The universal system with the same binding energy ratio as the LM2M2 potential would have the second excited tetramer state characterized by $B_4^{**}/B_3^* = 1.888(1)$ and $\Gamma/B_3^* = 0.0048(1)$. Comparison with direct LM2M2 results reveals quite sizable finite-range effects, especially for the resonance width that is twice as large as the universal prediction. The model dependence, estimated as the difference between LM2M2 and PCJS potential results, is considerably less significant. However, it becomes more visible for the resonance position in absolute values, i.e., $B_4^{**} = 4.14(4)$ mK for LM2M2 and $4.74(5)$ mK for PCJS, while the width is almost the same, $\Gamma = 0.023(2)$ mK and $0.024(2)$ mK, respectively.

Thus, although partially masked by higher waves, the second excited ^4He tetramer state should be observable in atom-trimer collisions as quite sharp resonance that is broadened due to finite range effects.

[1] V. Efimov, Phys. Lett. B **33**, 563 (1970).
 [2] M. Kunitski *et al.*, Science **348**, 551 (2015).
 [3] E. Braaten and H.-W. Hammer, Phys. Rep. **428**, 259 (2006).
 [4] P. Naidon and S. Endo, Reports on Progress in Physics **80**, 056001 (2017).
 [5] A. Kievsky, M. Gattobigio, L. Girlanda, and M. Viviani, Annual Review of Nuclear and Particle Science **71**, 465 (2021).
 [6] R. A. Aziz and M. J. Slaman, J. Chem. Phys. **94**, 8047 (1991).
 [7] M. Przybytek, W. Cencek, J. Komasa, G. Lach, B. Jeziorski, and K. Szalewicz, Phys. Rev. Lett. **104**, 183003 (2010).
 [8] D. Blume and C. H. Greene, J. Chem. Phys. **112**, 8053 (2000).
 [9] P. Barletta and A. Kievsky, Phys. Rev. A **64**, 042514 (2001).
 [10] R. Lazauskas and J. Carbonell, Phys. Rev. A **73**, 062717 (2006).
 [11] H. Suno and B. D. Esry, Phys. Rev. A **78**, 062701 (2008).
 [12] E. Kolganova, A. Motovilov, and W. Sandhas, Physics of Particles and Nuclei **40**, 206 (2009).
 [13] V. Roudnev and M. Cavagnero, J. Phys. B **45**, 025101 (2011).
 [14] T. K. Das, B. Chakrabarti, and S. Canuto, J. Chem. Phys. **134**, 164106 (2011).
 [15] E. Hiyama and M. Kamimura, Phys. Rev. A **85**, 022502 (2012).
 [16] A. Deltuva, Few-Body Syst. **56**, 897 (2015).
 [17] A. Deltuva, Phys. Rev. A **105**, 043310 (2022).
 [18] H. W. Hammer and L. Platter, Eur. Phys. J. A **32**, 113 (2007).
 [19] J. von Stecher, J. P. D’Incao, and C. H. Greene, Nature Phys. **5**, 417 (2009).
 [20] A. Deltuva, Phys. Rev. A **82**, 040701(R) (2010).
 [21] A. M. Badalyan, L. P. Kok, M. I. Polikarpov, and Y. A. Simonov, Phys. Rep. **82**, 31 (1982).
 [22] A. Deltuva, Europhys. Lett. **95**, 43002 (2011).
 [23] A. Deltuva, Few-Body Syst. **54**, 569 (2013).
 [24] M. Przybytek, W. Cencek, B. Jeziorski, and K. Szalewicz, Phys. Rev. Lett. **119**, 123401 (2017).
 [25] P. Grassberger and W. Sandhas, Nucl. Phys. **B2**, 181 (1967); E. O. Alt, P. Grassberger, and W. Sandhas, JINR report No. E4-6688 (1972).
 [26] O. A. Yakubovsky, Sov. J. Nucl. Phys. **5**, 937 (1967).
 [27] A. Deltuva and A. C. Fonseca, Phys. Rev. C **75**, 014005 (2007).
 [28] J. R. Taylor, *Scattering Theory* (John Wiley & Sons, Inc., New York, 1972).
 [29] A. Deltuva, Phys. Rev. A **85**, 012708 (2012).